Full Paper

Wiley Online Library

ELECTROANALYSIS

DOI: 10.1002/elan.201800068

Ordered Mesoporous Carbon/Poly (2-Hydroxyethyl Methacrylate/Ag Nanoparticle Composite Modified Glassy Carbon Electrode; an Amplified Sensor for Simultaneous Determination of Acetaminophen and Domperidone

Hamid Khoshsafar,[a] Mohammad Kazem Rofouei,*[a] Hasan Bagheri,[b] and Roozbeh Javad Kalbasi[a]

Abstract: In this study, we describe a modification of a glassy carbon electrode with an ordered mesoporous carbon (OMC)/poly (2-hydroxyethyl methacrylate) (PHEMA)/Ag nanoparticle composite (GCE/AgNPs-PHEMA-CMK-1) done for the first time and the application of a proposed sensor for the simultaneous determination of acetaminophen (AC) and domperidone (DO). The transmission electron microscopy (TEM), fourier-transform infrared spectroscopy (FT-IR), electrochemical impedance spectroscopy (EIS), UV-vis spectroscopy, and X-ray powder diffraction (XRD) methods were used for the analysis of the synthesized nanocomposite. The GCE/AgNPs-PHEMA-CMK-1 showed good catalytic activity for the electro-oxidation of acetaminophen and domperidone in the buffer solution. The pH investigation showed that acetaminophen and domperidone electro-oxidation is relative to the pH value of the solution. The maximum oxidation process occurred at pH = 7.0 and pH = 8.0 for acetaminophen and domperidone, respectively, on the surface of the GCE/AgNPs-PHEMA-CMK-1. The GCE/AgNPs-PHEMA-CMK-1 showed a linear range between 0.015–7.5 μM and 0.03–10.8 μM for acetaminophen and domperidone, respectively. The GCE/AgNPs-PHEMA-CMK-1 showed detection limits of 0.005 and 0.01 μM for acetaminophen and domperidone, respectively, by the differential pulse voltammetry (DPV) method. Finally, the GCE/AgNPs-PHEMA-CMK-1 was suggested as a highly powerful tool for the analysis of acetaminophen and domperidone in real samples.

Keywords: Ordered mesoporous carbon · Acetaminophen · Domperidone · Ag nanoparticle · Sensor

1 Introduction

The determination of drugs in blood, tablet, and urine samples is very important due to their high consumption and many destructive side effects [1–5]. The need for sensitive and selective analytical sensors for the detection of pharmaceutical compounds has increased. This is due to the significant growth of medication intake for the treatment of the human body and also because of the variety of drugs available [6]. Some years ago, high-performance liquid chromatography methods were suggested due to the low limit of detection and the wide range application for drug analysis [7–9]. However, the relative signal to operator skill, using toxic solvents, and a long time for analysis are the main disadvantages of this type of analytical method for pharmaceutical analysis. In recent years, modified electrochemical sensors and modified voltammetric sensors were used extensively for the analysis of different types of electroactive materials and especially, pharmaceutical compounds [10–14]. Fast response analysis, low toxicity, and high sensitivity are the main advantages of using electrochemical modified sensors for the analysis of electro-active materials [15–18].

Acetaminophen is a useful and widely used drug for treating pain, muscle aches, headache, arthritis, colds, and fevers [19,20]. Although acetaminophen is often suggested for the treatment of patients, an overdose with this drug can damage the liver or even cause death. Therefore, many analytical sensors were suggested for the determination and control of acetaminophen in urine and blood samples [21–23].

Domperidone is a dopamine D_2 receptor antagonist drug for the treatment of gastroesophageal reflux disease (GERD), nausea, and vomiting [24]. A combination of domperidone and acetaminophen can be useful in the treatment of migraines. The simultaneous determination of these drugs is very important in biological samples [25].

Ordered mesoporous carbons have received substantial attention because of their large pore volume, good uniform conductivity, narrow pore size distribution, high specific surface area, and chemical inertness. Furthermore,

[a] H. Khoshsafar, M. K. Rofouei, R. J. Kalbasi
Faculty of Chemistry, Kharazmi University, Tehran, Iran
E-mail: rofouei@khu.ac.ir
[b] H. Bagheri
Chemical Injuries Research Center, Systems Biology and Poisonings Institute, Baqiyatallah University of Medical Sciences, Tehran, Iran

Supporting information for this article is available on the WWW under https://doi.org/10.1002/elan.201800068

they have low background current and a wide window of potential that makes them suitable for electroanalytical and catalytic applications [26,27].

The use of nanomaterials is widespread in different areas, such as chemical and biological sensing, medical diagnostics, and therapeutics. From a structural perspective, metal nanoparticles have various optical, magnetic, electronic, and catalytic properties. In electrochemical applications, metal nanoparticles provide some special functions, such as catalytic and conductivity properties, and the roughening of the conductive sensing interface. The incorporating of metal nanoparticles on the surface of OMCs further improves its performance and provides properties such as high conductivity and desirable electrochemical activity [28–30].

Domperidone and acetaminophen possess amide and hydroxyl functional groups and there are carbonyl groups on the surface of the PHEMA. Therefore, the hydrogen bonding formation between these groups can take place. The presence of these interactions may increase the accumulated amount of the analytes on the electrode surface and lead to higher responses [31].

Due to the important analysis of domperidone and acetaminophen and the high performance of electrochemical methods for drug analysis, in this research, we fabricated a highly sensitive voltammetric sensor based on a glassy carbon electrode modified with an ordered mesoporous carbon/poly (2-hydroxyethyl methacrylate)/Ag nanoparticle composite for the simultaneous determination of domperidone and acetaminophen in aqueous solutions.

2 Experimental

2.1 Materials

For the synthesis of the AgNPs/PHEMA/CMK-1, cetyltrimethylammonium bromide (CTAB), tetraethylorthosilicate (TEOS), ethanol, sulfuric acid, sucrose, 2-hydroxyethyl methacrylate, tetrahydrofuran (THF), benzoyl peroxide, ammonia, and domperidone were purchased from Sigma-Aldrich. Silver nitrate ($AgNO_3$), sodium borohydride ($NaBH_4$), and acetaminophen were purchased from Merck. The phosphate buffer solution (PBS, 0.1 M) was prepared with sodium dihydrogen phosphate and disodium monohydrogen phosphate; the pH value was adjusted with HCl or NaOH.

2.2 Apparatus

For the electrochemical investigation, an Autolab 302 N coupled with the electrochemical cell in the presence of the $Ag/AgCl/KCl_{sat}$ (reference electrode), modified and unmodified glassy carbon electrodes (working electrodes), and platinum (counter electrode) were used. The transmission electron microscope (TEM) observations were performed on a JEOL JEM.2011. The X-ray patterns were achieved by a Bruker D8Advance. The samples were analyzed using the FT-IR spectroscopy (using a PerkinElmer 65 in KBr matrix in the range of 4000–400 cm^{-1}). The absorption spectra of samples were obtained by UV-vis spectrometer (Lamda 750 UV/vis/NIR Spectrophotometer, Perkin-Elmer). The determination of the amount of Ag nanoparticles was carried out on an ICP-OES (Varian Vista-Pro).

2.3 Synthesis of AgNPs-PHEMA-CMK-1

The CMK-1 was synthesized, according to our previous papers [15,32]. In the first step, we synthesized CMK-1 by the following procedure. A 50 mL CTAB 0.13 M was prepared and mixed with 50 mL ethanol and 12 mL ammonia by stirring continuously for 10 min. Then 16 mmol TEOS as a silica source was added to the previous solution and stirred for 2 h. The precipitated washed with double distilled water for sometime, and MCM-48 was obtained after calcination.

In the second step, 5 mL sucrose (0.73 M) was added to a flask in the presence of 1.0 g MCM-48 and 76 μL sulfuric acid. The obtained mixture was heated under temperature programming. This stage of the experiment was repeated to obtain completely polymerized sucrose inside the pores of the MCM-48 template. It was then put in a furnace at 900 °C under a nitrogen atmosphere for 6 h. The black product was then washed twice with an alcoholic NaOH solution (1 M), filtered, and dried. The mesoporous carbon CMK-1 was obtained as OMC.

In the third step, 2-hydroxyethyl methacrylate (0.5 mL; 4.12 mmol) and 0.5 g CMK-1 was dissolved in 7.0 mL THF in a round-bottom flask. The benzoyl peroxide (3 mol%; 0.029 g) was added to the mixture and stirred for 5 h under a nitrogen atmosphere at 65–70 °C, the black product, PHEMA/CMK-1, was washed with THF a few times, and then dried at 60 °C.

In the final step, the AgNPs-PHEMA-CMK-1 was synthesized by the reduction of silver nitrate in the presence of $NaBH_4$ as a reducing agent. An appropriate amount of PHEMA-CMK-1 was dispersed in 10 mL $AgNO_3$ (0.01 M) and reflux for 2 h and then cooled to ambient temperature; after that the mixture sonicated for 15 min. Then the solution was put in an ice bath, and 20 mL of $NaBH_4$ (0.05 M) was slowly (one drop per second) added under vigorous stirring. The product was dried in an oven at 50 °C. The Ag content of the composite was estimated by the inductively coupled plasma optical emission spectrometry (ICP-OES) after decomposing the known amount of the composite by perchloric acid, nitric acid, fluoric acid, and hydrochloric acid.

2.4 Construction of GCE/AgNPs-PHEMA-CMK-1

The glassy carbon electrode was polished with alumina powder (0.1 μm) and then sonicated for 5 min with methanol and doubly-distilled water, respectively. For the construction of the sensor, 5 mg AgNPs-PHEMA-CMK-1

was dispersed in 10 mL N, N-dimethylformamide with 15 min continuous ultrasonication. Then 5 μL synthesized modifier was added on the surface of the glassy carbon electrode and dried with an IR (infrared) lamp.

2.5 Real Sample Preparation

In order to evaluate the practicality of the proposed sensor for the voltammetric determination of acetaminophen and domperidone in real samples, the recovery of which were determined in domperidone tablet, acetaminophen tablet, serum, and urine samples.

For the determination of the acetaminophen and domperidone in the urine samples, the collected urine was centrifuged for 45 min at 2000 rpm. The supernatant was filtered using a 0.45 μm filter and then diluted ten times with PBS.

Drug-free human serum samples were obtained from volunteers (healthy persons) and stored in a refrigerator immediately after collection until the time of analysis. Due to the possibility of protein bonding for acetaminophen and domperidone and reducing the recovery process, it was necessary to conduct some treatments with plasma before the analysis. Acetonitrile removes serum proteins more effectively and is used as a serum-precipitating agent; the mixture was centrifuged at 6000 rpm for 30 min. The supernatant was filtered carefully through a cellulose acetate filter (0.2 μm pore size, Advantec MFS, CA) and then diluted five times with PBS at pH 8 and spiked with exogenous acetaminophen and domperidone. The solution was transferred into the volumetric cell to be analyzed without any further pretreatment.

Ten acetaminophen and domperidone tablets were crushed separately by a mortar and pestle and homogenized. A mass of powders equivalent to the average mass of one tablet was weighed and transferred to 100 mL volumetric flasks. The flasks sonicated for 10 min and was then filled with the PBS. After complete dissolution, the solution was filled on an ordinary filter paper. An appropriate volume of stock solutions was transferred into the volumetric cells for analysis.

3 Results and Discussion

3.1 Characterization of Synthesized AgNPs-PHEMA-CMK-1 Nanocomposite

The CMK-1 and PHEMA-CMK-1 nanocomposite was characterized by the TEM method. Figure 1a and b shows the TEM images of CMK-1 and PHEMA-CMK-1, respectively. In these figures, an ordered mesoporous structure of CMK-1 and PHEMA-CMK-1 can be detected. In addition, after the modification of the PHEMA-CMK-1 with the Ag nanoparticle, we observed Ag nanoparticles on the surface of the PHEMA-CMK-1 with uniform distribution (Figure 1c). Furthermore, the size distribution of AgNPs in AgNPs-PHEMA-CMK-1 was

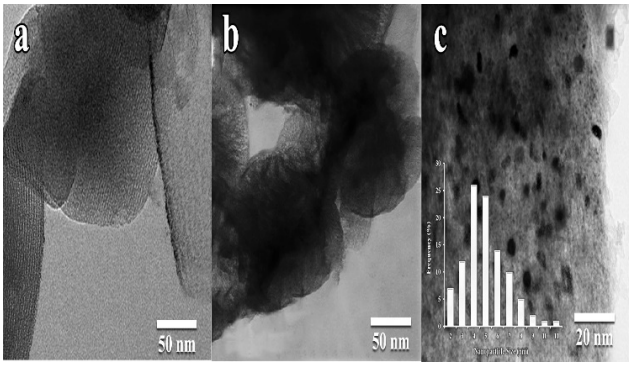

Fig. 1. TEM images of (a) CMK-1, (b) PHEMA-CMK-1 and (c) AgNPs-PHEMA-CMK-1, inset shows corresponding size distribution of Ag nanoparticles.

measured. As shown in Figure 1(c) (inset) the size distribution is narrow with an average size of 4.3 nm.

The X-ray powder diffraction (XRD) method was used for the investigation of the synthesized powders. The XRD patterns are presented in Figure S1 (Supporting Information). As can be seen in the wide-angle XRD pattern of the AgNPs-PHEMA-CMK-1 nanocomposite ($2\Theta = 10–90^\circ$), some intense peaks at $2\Theta = 37.9$, 44.1, 64.2, 77.6° can be seen which are related to Ag nanoparticles on the surface of the composite. Also, the XRD pattern of the CMK-1, PHEMA-CMK-1, and AgNPs-PHEMA-CMK-1 in the 2θ range (2–8°) are presented in Figure S1 (inside). All the samples showed similar XRD patterns which indicate that the ordered structure of CMK-1 is retained even after incorporation of polymers and Ag nanoparticles on it.

The FT-IR spectra of the CMK-1 (a), PHEMA/CMK-1 (b), and Ag-PHEMA/CMK-1 (c) are shown in Figure S2. As can be seen, a broad band at about 3400 cm^{-1} is observed in all the samples. It is related to the OH stretching vibration. The appearance of new peaks in the FT-IR spectrum of the PHEMA/CMK-1 confirmed the successful synthesis of the PHEMA/CMK-1. A band at about 1729 cm^{-1} assigned to the C=O bond in the polymer structure [33] and the broad band at around 3000 cm^{-1} is attributed to aliphatic CH stretching vibration.

Moreover as shown in the Ag-PHEMA/CMK-1 spectrum (Figure S2), the redshift takes place and the band around 1725 cm^{-1} is shifted to lower values (1711 cm^{-1}). Furthermore, the peak intensity is decreased. This may be due to the interaction between the carbonyl groups and the Ag nanoparticles indicating the presence of Ag on the surface of the PHEMA.

In order to provide more accurate evidence on the formation of Ag nanoparticles, the UV-vis absorption spectra of materials were recorded and appear in Figure S3. UV-vis measurements have been proved to be quite sensitive to the formation of Ag nanoparticles because AgNPs exhibit an intense absorption peak due to the surface Plasmon excitation. Figure S3 shows the UV-vis spectra of AgNPs-CMK-1 and AgNPs-PHEMA-CMK-

1. The absorption band observed at 400 nm in both samples is attributed to the absorption of Ag nanoparticles. PHEMA and CMK-1 showed no absorbance in the UV-vis region.

3.2 The Electrical Conductivity of AgNPs-PHEMA-CMK-1 at a Surface of Sensor

Electrochemical impedance spectroscopy (EIS) is a suitable technique for investigating of the electrode surface dependent charge transfer process (interfacial properties, i.e., resistance and capacitance). The curve of the EIS includes a semicircular part and a linear part. The semicircular part at higher frequencies corresponds to the electron-transfer-limited process and its diameter is equal to the electron transfer resistance, which controls the electron transfer kinetics of the redox probe at the electrode interface. The measurements are generally performed in Faradaic mode in frequency range 0.1–100000 Hz, using redox-probe ferrocyanide/ferricyanide in order to focus on the variations of the charge transfer resistance (it is equal to the semicircle diameter) between the solution and the electrode surface. The equivalent circuit compatible with the Nyquist diagram recorded for fabricated sensor is depicted in Figure 2. In this circuit, R_s, C_{dl} and R_{ct} represent solution resistance, a capacitance for the double-layer and charge transfer resistance, respectively. W is a finite-length Warburg short-circuit term coupled to R_{ct}, which accounts for the Nernstian diffusion. This equivalent circuit (Figure 2 inset) was used to fit the impedance spectra and extract the values of C_{dl} and R_{ct}. After the modification of the electrode composition with various specific materials, the value of R_{ct} changes, due to their conduction properties. By monitoring the value of R_{ct} after each modification step in electrode composition, most sensitive sensing layer can be selected with remarkable accuracy. Figure 2 illustrated the impedance spectra observed at each step in the presence of 1.0 mmol L^{-1} $Fe(CN)_6^{3-/4-}$ solution.

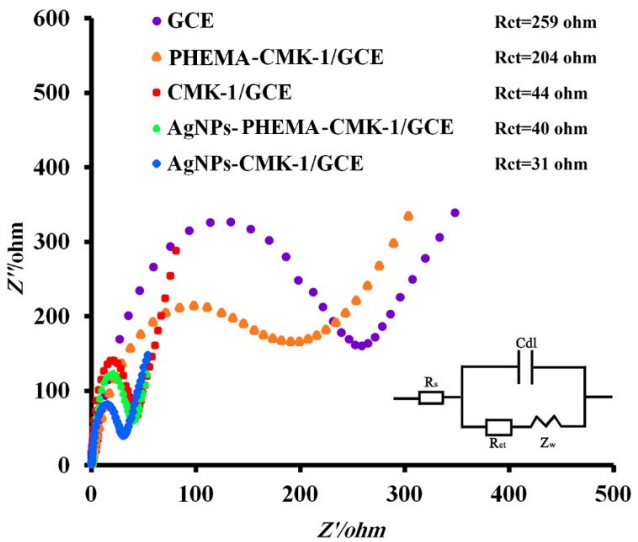

Fig. 2. Nyquist plots for various prepared electrodes in the 1.0 mmol L^{-1} $[Fe(CN)_6]^{3-/4-}$ and 0.1 mol L^{-1} KCl.

As shown in Figure 2, when GCE was unmodified, the semicircle associated with R_{ct} increased obviously, suggesting that GCE has a low rate of electron transfer due to its poor conductivity (259 Ω). However, after GCE was modified with CMK-1, the R_{ct} value decreased distinctively to 44 Ω indicating that CMK-1 could accelerate the electron transfer between the electrochemical probe $[Fe(CN)_6]^{3-/4-}$ and the electrode surface. As can be seen in Figure 2, the impedance plot of AgNPs-CMK-1/GCE involves an extremely small radius, smaller than those of other electrodes. A large decrease in charge-transfer resistance of AgNPs-CMK-1/GCE is definitely due to the high conductivity and remarkable surface area of Ag nanoparticle and CMK-1. At PHEMA-CMK-1/GCE, the R_{ct} increased to 204 Ω, indicating that the PHEMA formed an additional barrier on the surface of electrode to block the electron exchange between the solution and the electrode. This is due to the fact that the polymeric modifier was not conductive. However, the accumulation of analytes at the electrode surface is mainly affected by the interaction between analytes and PHEMA. Thus, the voltammetric responses of AC and DO are closely related to the presence of PHEMA in the modified electrode. When the electrode was modified with AgNPs-PHEMA-CMK-1, the Rct decreased (40 ohm)

in comparison with PHEMA-CMK-1/GCE. This was attributed to that the coating of PHEMA-CMK-1 surface with Ag nanoparticles increased the ability of the redox probe to electron transfer. On the other hand, we detected active surface areas of 0.060 cm^2, 0.069 cm^2, 0.085 cm^2, 0.062 cm^2, and 0.066 cm^2 for GCE, GCE/CMK-1, GCE/AgNPs-CMK-1, GCE/PHEMA-CMK-1, and GCE/AgNPs-PHEMA-CMK-1, respectively, in the presence of 1.0 mM of $K_4Fe(CN)_6$ and based on the Randles-Sevcik equation.

3.3 Effect of the Amount of Ag Nanoparticles

The electrochemical response of the modified electrode towards acetaminophen and domperidone strongly depends on the amount of Ag nanoparticles on the PHEMA-CMK-1. The peak current increases by increasing the amount of Ag until 2%; then it remains almost constant; current decline takes place above 4% (Figure S4). This decrease can be related to the reduction of the available PHEMA-CMK-1 cavity and consequently, a reduction of the surface area. Therefore, the AgNPs-PHEMA-CMK-1 nanocomposite with an Ag loading amount of 2 wt% is selected as a modifier for the construction of a sensor for the analysis of acetaminophen and domperidone.

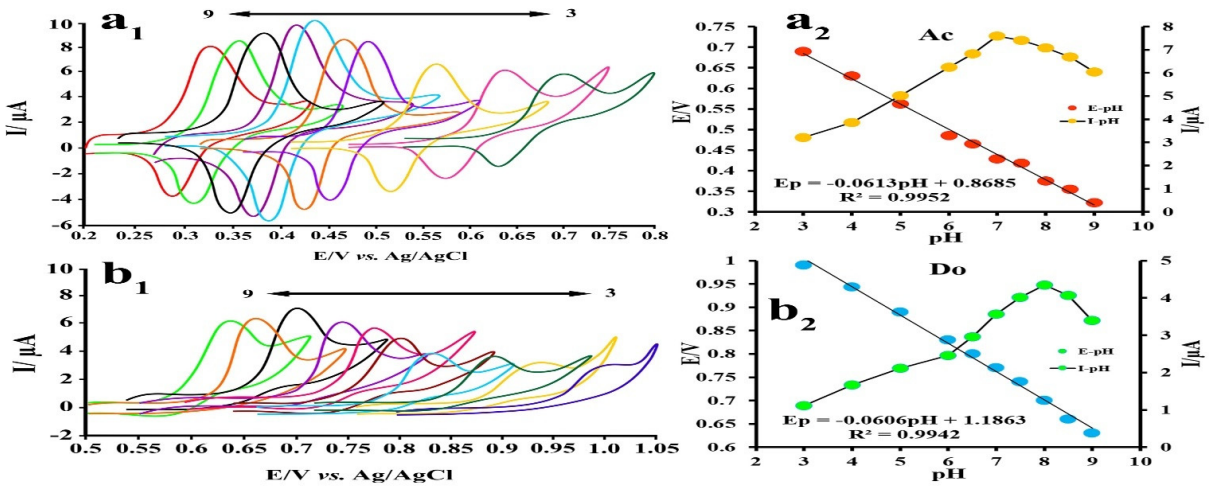

Fig. 3. Cyclic voltammograms of GCE/AgNPs-PHEMA-CMK-1 containing 5 μM AC (a_1) and 10 μM DO (b_1) in various pHs (3.0, 4.0, 5.0, 6, 6.5, 7.0, 7.5, 8, 8.5 and 9.0) Scan rate, 100 mV s^{-1}. Effect of pH on the anodic peak currents and potentials of AC (a_2) and DO (b_2).

3.4 Electro-Oxidation Behavior of Acetaminophen and Domperidone at a Surface of Proposed Sensor

According to previously published papers and the structure of acetaminophen and domperidone [33–36], we found that the electro-oxidation behavior of these drugs is relative to the pH of the solution; this factor is optimized in the first step. The cyclic voltammograms of 5 μM acetaminophen (Figure 3 a_1) and 10 μM domperidone (Figure 3 b_1) were recorded at a different pH on the surface of the GCE/AgNPs-PHEMA-CMK-1. As can be seen, the maximum oxidation current occurred at pH = 7.0 (Figure 3 a_2) for acetaminophen and pH = 8.0 for domperidone (Figure 3 b_2), respectively. According to the obtained data, we selected pH = 8.0 for the simultaneous analysis of acetaminophen and domperidone due to the high affinity of the sensor to acetaminophen compared to domperidone and a good response of the sensor to domperidone at pH = 8.0. The relation between the peak potential and the pH for the electro-oxidation of acetaminophen and domperidone are shown in Figure 3 a_2 and Figure 3 b_2. The obtained slopes are near to the Nernstian value that confirmed the equal value of proton and electron in the oxidation mechanism of two drugs (see Figure 3 a_2 and b_2).

The electro-oxidation behavior of acetaminophen and domperidone were investigated on the surfaces of the GCE, GCE/CMK-1, GCE/AgNPs-CMK-1, GCE/PHEMA-CMK-1, and GCE/AgNPs-PHEMA-CMK-1; the obtained data are presented in Figure 4a and b. When moving from the GCE to the GCE/AgNPs-PHEMA-CMK-1, the oxidation current of the two drugs increased, and the over-potential for their electro-oxidation reduced. The active surface area of the GCE/AgNPs-CMK-1 is more than the active surface area of the GCE/AgNPs-PHEMA-CMK-1 and the conductivity of the GCE/AgNPs-CMK-1 is better than the GCE/AgNPs-PHEMA-CMK-1. However, the affinity of the PHEMA to acetaminophen and domperidone due to the functional groups of polymer to drugs improved the sensitivity of the sensor for the simultaneous analysis of acetaminophen and domperidone.

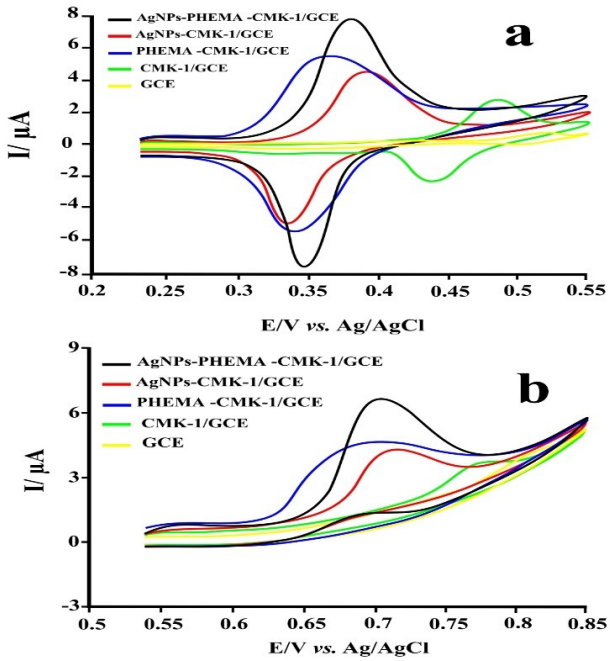

Fig. 4. Cyclic voltammograms of 5 μM AC (a) and 10 μM DO (b) with a scan rate of 100 mV s^{-1} in PBS (pH 8) on the surface of various electrodes.

Furthermore the cyclic voltammogram of the AgNPs/GCE in PBS (pH 8) in the absence of analyte is presented in Figure S5 (curve a), the anodic peak corresponds to the $Ag \rightarrow Ag^+$ process, while the cathodic peak represents the

cathodic counterpart of this process. The curve b shows the response of AgNPs-CMK-1/GCE in the absence of analyst. As can be seen, when the Ag nanoparticle was deposited on the CMK-1 surface, the redox peaks disappeared.

In addition cyclic voltammogram of the AgNPs-PHEMA-CMK-1/GCE in the absence of AC and DO is shown as curve c in Figure S5. As can be seen, there is no electrochemical peak wave is observed on this electrode, indicating the absence of electrochemical activity. This clearly demonstrates that, the origin of the electrochemical activity, in our experiment, is due to the AC and DO.

The scan rate effect for the electro-oxidation of acetaminophen and domperidone were investigated on the surface of the GCE/AgNPs-PHEMA-CMK-1 (Figure 5a and b). The linear relation can be observed between the oxidation currents of acetaminophen and domperidone (Figure 5 a_1 and b_1) and $\nu^{1/2}$; this confirms the diffusion process for the electro-oxidation of the drugs on the surface of the GCE/AgNPs-PHEMA-CMK-1.

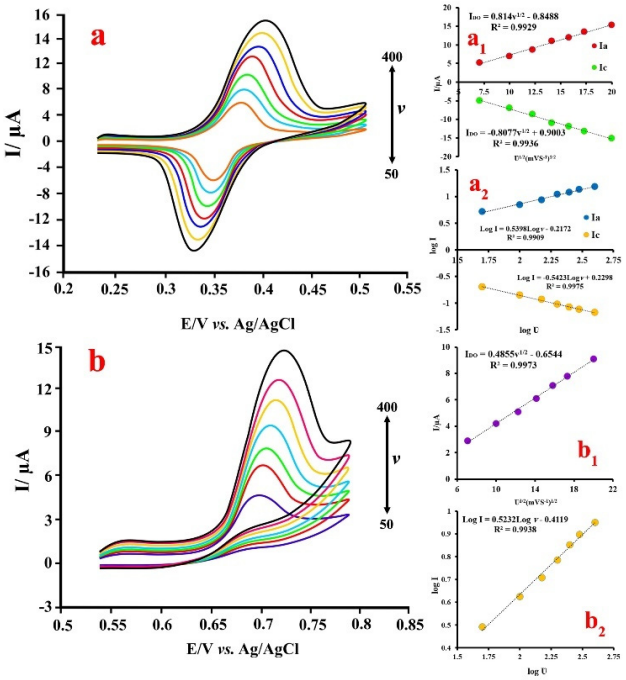

Fig. 5. Cyclic voltammograms of GCE/AgNPs-PHEMA-CMK-1 containing 5 µM AC (a) and 10 µM DO (b) in PBS (pH 8.0) with scan rate ranging from 50 to 400 mV s^{-1}. The linear relationship of the anodic peak current of AC (a_1) and DO (b_1) versus square root of the scan rate ($\nu^{1/2}$). The linear relationship of the Log (I_p) of AC (a_2) and DO (b_2) versus Log (ν).

In addition, a linear relationship between log I_p and log ν of acetaminophen and domperidone are presented in Figure 5 a_2 and Figure 5 b_2, respectively. The slope values were comparable with the theoretical value of 0.5, which is expressed for an ideal reaction of diffusion controlled electrode process.

3.5 Simultaneous Determination of Acetaminophen and Domperidone

The differential pulse voltammetric method was used for the determination of acetaminophen and domperidone on the surface of the GCE/AgNPs-PHEMA-CMK-1 (Figure 6). The DPVs showed two separated oxidation signals in the concentration range of 0.015–7.5 µM (sensitivity: 2.406 µA/µM) and 0.03–10.8 µM (sensitivity: 0.941 µA/µM) with detection limits of 0.005 µM and 0.01 µM for acetaminophen and domperidone, respectively.

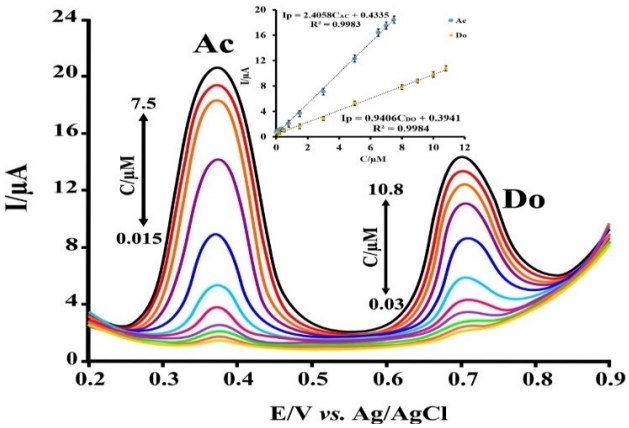

Fig. 6. DPVs of GCE/AgNPs-PHEMA-CMK-1 containing different concentrations of AC and DO in PBS (pH 8.0).

On the other hand, the DPVs of acetaminophen in the presence of a fixed concentration of domperidone (5.0 µM) showed a sensitivity of 2.421 µA/µM, which is very similar to the obtained sensitivity from the analysis of acetaminophen in the presence of different concentrations of domperidone (Figure 7a).

In addition, with a change in the concentration of acetaminophen, the oxidation signal of domperidone was made fix, which confirms that there was no interaction between acetaminophen and domperidone on the surface of the GCE/AgNPs-PHEMA-CMK-1. Also, a similar data was observed for different concentrations of domperidone in the presence of a fixed amount of acetaminophen (Figure 7b).

The comparison between the proposed method and other reported sensors for the determination of acetaminophen and domperidone was shown in Table S1. Clearly, the proposed methods are simple with comparable and even more sensitive in terms of LOD than the other reported methods. Furthermore the oxidation peaks in this work appear in the potentials lower than most of the other reports which shows good electrocatalitic activity of the proposed sensor.

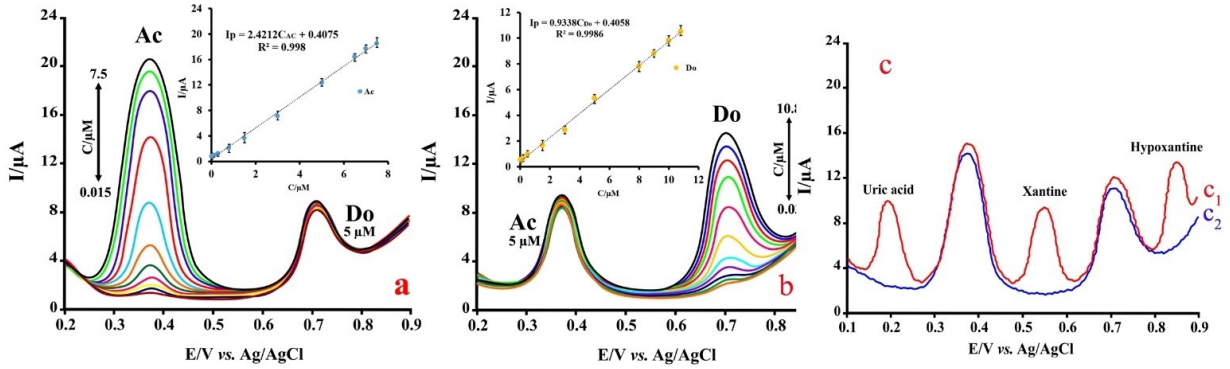

Fig. 7. (a) DPVs for AC at the GCE/AgNPs-PHEMA-CMK-1 in the presence of 5 μM DO in PBS (pH 8.0). AC concentrations: 0.015, 0.025, 0.1, 0.3, 0.8, 1.5, 3, 5, 6.5, 7 and 7.5 μM. (b) DPVs for DO at the GCE/AgNPs-PHEMA-CMK-1 in the presence of 5 μM AC. DO concentrations: 0.03, 0.05, 0.2, 0.5, 1.5, 3, 5, 8, 9, 10 and 10.8 μM. DPVs of oxidation of 5 μM acetaminophen and 8 μM domperidone in phosphate buffer solution (pH 8.0) in the absence (c2) and presence of 80 μM uric acid, 100 μM xanthine and 100 μM hypoxanthine (c1).

3.6 Interference Study and Stability of GCE/AgNPs-PHEMA-CMK-1

The long-term stability of the GCE/AgNPs-PHEMA-CMK-1 was evaluated in the presence of acetaminophen and domperidone.

The oxidation peak currents of acetaminophen and domperidone were reduced by less than 3.8% after four cycles, without any change in the peak potential. Also, the differential pulse voltammograms showed minimal change after storing the sensor in a bottle for 35 days over the PBS (pH = 8.0).

The selectivity of the GCE/AgNPs-PHEMA-CMK-1 was checked for the analysis of analytes at a pH = 8.0. The concentration of foreign species, which leads to a relative error less than 5% for the determination of 5 μM acetaminophen and 8 μM domperidone was considered as the tolerance limit.

The result demonstrated that, under optimal conditions, 700 fold of K^+, CO_3^{2-}, Cl^-, SO_4^{2-}, Na^+, NH_4^+, Ca^{2+}, Mg^{2+}, NO^{3-}; 400 fold of cysteine, arginine, histidine; 250 fold of glucose, lactose, sucrose, fructose and 10 fold excess of dopamine did not show any interferences for the analysis of acetaminophen and domperidone on the surface of the GCE/AgNPs-PHEMA-CMK-1. In addition, the effect of 80 μM uric acid, 100 μM xanthine, and 100 μM hypoxanthine on the voltammetric response of acetaminophen and domperidone was investigated. No noticeable change in the peak currents of acetaminophen and domperidone were observed, and the peaks of analytes were well separated from the peaks of the interfering species, verifying the applicability of the GCE/AgNPs-PHEMA-CMK-1 for the simultaneous determination of acetaminophen and domperidone in the presence of these compounds. Figure 7c shows the DPVs of oxidation of 5 μM acetaminophen and 8 μM domperidone in PBS (pH 8.0) in the absence (Figure 7 c_2) and presence of 80 μM uric acid, 100 μM xanthine, and 100 μM hypoxanthine (Figure 7 c_1)

3.7 Real Sample Analysis of Acetaminophen and Domperidone

The ability of GCE/AgNPs-PHEMA-CMK-1 was checked for analysis of acetaminophen and domperidone in some biological and pharmaceutical samples. The standard addition method was used for the investigation of the sensor in a real sample analysis of acetaminophen and domperidone. The results obtained are given in Table 1. Each value is an average of four measurements. As shown in Table 1, the recovery values were in the range of 98.3–102.4% and 98.1–102.5% for the acetaminophen and domperidone tablets, respectively. Also, the RSD% value was below 5% for both samples. The presented data in Table 1 confirmed the high-performance ability of the GCE/AgNPs-PHEMA-CMK-1 as a new electrochemical sensor for acetaminophen and domperidone analysis in real samples.

4 Conclusion

In this study, a novel and highly sensitive electrochemical sensor was constructed based on a glassy carbon electrode modified with an ordered mesoporous carbon/poly (2-hydroxyethyl methacrylate)/Ag nanoparticle composite. The GCE/AgNPs-PHEMA-CMK-1 showed high catalytic activity for the electro-oxidation of acetaminophen and domperidone in the mixed samples. In addition, the GCE/AgNPs-PHEMA-CMK-1 showed two separated oxidation signals for acetaminophen and domperidone with limits of detection of 0.005 and 0.01 μM, respectively. Finally, the GCE/AgNPs-PHEMA-CMK-1 was used for the analysis of acetaminophen and domperidone in the real samples.

Table 1. Determination results of AC and DO in real samples obtained by the proposed method under the optimum conditions.

Sample	Added(μM)		Found(μM)		Recovery (%)	
	AC	DO	AC	DO	AC	DO
Urine	0	0	< detection limit	< detection limit	–	–
	2	2	2.02	2.05	101.0	102.5
	5	5	5.12	4.94	102.4	98.8
	7	10	6.92	9.91	98.9	99.1
Serum	0	0	< detection limit	< detection limit	–	–
	2	2	1.97	1.97	98.5	98.5
	5	5	5.04	5.09	100.8	101.8
	7	10	6.88	10.02	98.3	100.2
AC tablet[a]	0	0	1.97	< detection limit	98.5	–
	1	2	2.95	1.98	98.3	99.0
	3	5	4.97	5.12	99.4	102.4
	5	10	6.94	10.05	99.1	100.5
DO tablet[b]	0	0	< detection limit	4.07	–	101.8
	4	3	3.99	6.87	99.8	98.1
	7	6	7.04	9.83	100.6	98.3

[a]Samples of AC tablets are presented in the concentration of 2 μM. [b]Samples of DO tablets are presented in the concentration of 4 μM.

Acknowledgments

The authors gratefully acknowledge the support of this work by the Kharazmi University, Tehran, Iran.

References

[1] M. H. Mashhadizadeh, N. Naseri, M. A. Mehrgardi, *Analytika* **2016**, *8*, 7247–7253.
[2] H. Bagheri, A. Shirzadmehr, M. Rezaei, H. Khoshsafar, *Ionics* **2017**, 1–11.
[3] H. Khoshsafar, H. Bagheri, M. Rezaei, A. Shirzadmehr, A. Hajian, Z. Sepehri, *J. Electrochem. Soc.* **2016**, *163*, B422-B427.
[4] H. Karimi-Maleh, F. Amini, A. Akbari, M. Shojaei, *J. Colloid Interface Sci.* **2017**, *495*, 61–67.
[5] B. J. Sanghavi, P. K. Kalambate, S. P. Karna, A. K. Srivastava, *Talanta* **2014**, *120*, 1–9.
[6] J. Trontelj, T. Vovk, M. Bogataj, A. Mrhar, *Pharmacol. Res.* **2005**, *52*, 334–339.
[7] M. Kamberi, K. Tsutsumi, T. Kotegawa, K. Nakamura, S. Nakano, *Clinical chemistry* **1998**, *44*, 1251–1255.
[8] D. E. Breithaupt, *Food Chem.* **2001**, *74*, 521–525.
[9] K. Basavaiah, U. Anil Kumar, K. Tharpa, *Acta Pharm.* **2008**, *58*, 347–356.
[10] F. Tahernejad-Javazmi, M. Shabani-Nooshabadi, H. Karimi-Maleh, *Talanta* **2018**, *176*, 208–213.
[11] A. C. Torres, M. M. Barsan, C. M. Brett, *Food Chem.* **2014**, *149*, 215–220.
[12] L. V. Tarditto, F. J. Arévalo, M. A. Zon, H. G. Ovando, N. R. Vettorazzi, H. Fernández, *Microchem. J.* **2016**, *127*, 220–225.
[13] M. L. Yola, T. Eren, N. Atar, *Biosens. Bioelectron.* **2014**, *60*, 277–285.
[14] N. F. Atta, M. F. El-Kady, *Sens. Actuators B* **2010**, *145*, 299–310.
[15] M. K. Rofouei, H. Khoshsafar, R. J. Kalbasi, H. Bagheri, *RSC Adv.* **2016**, *6*, 13160–13167.
[16] H. Karimi-Maleh, A. F. Shojaei, K. Tabatabaeian, F. Karimi, S. Shakeri, R. Moradi, *Biosens. Bioelectron.* **2016**, *86*, 879–884.
[17] P. Audebert, N. Vila, C. Allain, F. Maisonneuve, A. Walcarius, P. Hapiot, *ChemElectroChem* **2015**, *2*, 1695–1698.
[18] D. Sun, H. Zhang, *Microchim. Acta* **2007**, *158*, 131–136.
[19] H. Ueda, R. Pereira-Rosario, C. Riley, J. Perrin, *J. Pharm. Biomed. Anal.* **1989**, *7*, 309–320.
[20] E. Ziemons, J. Mantanus, P. Lebrun, E. Rozet, B. Evrard, P. Hubert, *J. Pharm. Biomed. Anal.* **2010**, *53*, 510–516.
[21] A. Afkhami, H. Khoshsafar, H. Bagheri, T. Madrakian, *Anal. Chim. Acta* **2014**, *831*, 50–59.
[22] F. Valentini, E. Ciambella, F. Cataldo, A. Calcaterra, L. Menegatti, M. Talamo, *Electroanalysis* **2017**, *29*, 2863–2872.
[23] X. Kong, Y. Wang, Q. Zhang, T. Zhang, Q. Teng, L. Wang, H. Wang, Y. Zhang, *J. Colloid Interface Sci.* **2017**, *505*, 615–621.
[24] F. Marchetti, M. Bonati, A. Maestro, D. Zanon, F. Rovere, A. Arrighini, E. Barbi, P. Bertolani, P. Biban, L. Da Dalt, *PLoS One* **2016**, *11*, e0165441.
[25] E. A. MacGregor, M. Wilkinson, K. Bancroft, *Cephalalgia* **1993**, *13*, 124–127.
[26] J. C. Ndamanisha, L.-p. Guo, *Anal. Chim. Acta* **2012**, *747*, 19–28.
[27] A. Walcarius, *Sensors* **2017**, *17*, 1863.
[28] B. Li, T. Zhang, H. Wang, X. Zhao, F. Li, M. Liu, J. Zhao, Y. Zhang, *RSC Adv.* **2016**, *6*, 93469–93475.
[29] X. Bo, J. Bai, L. Yang, L. Guo, *Sens. Actuators B* **2011**, *157*, 662–668.
[30] A. Korani, A. Salimi, B. Karimi, *Electroanalysis* **2017**, *29*, 2646–2655.
[31] L. Bounabi, N. B. Mokhnachi, N. Haddadine, F. Ouazib, R. Barille, *J. Drug Delivery Sci. Technol.* **2016**, *33*, 58–65.
[32] R. J. Kalbasi, N. Mosaddegh, *Catal. Commun.* **2011**, *12*, 1231–1237.
[33] P. Y. Khashaba, H. R. H. Ali, M. M. El-Wekil, *Materials Science and Engineering: C* **2017**, *75*, 733–741.
[34] P. K. Kalambate, B. J. Sanghavi, S. P. Karna, A. K. Srivastava, *Sens. Actuators B* **2015**, *213*, 285–294.
[35] R. N. Goyal, *Talanta* **2015**, *141*, 53–59.
[36] S. Cheraghi, M. A. Taher, H. Karimi-Maleh, *Electroanalysis* **2016**, *28*, 366–371.

Received: January 30, 2018
Accepted: July 23, 2018
Published online on ■■, ■■■

FULL PAPER

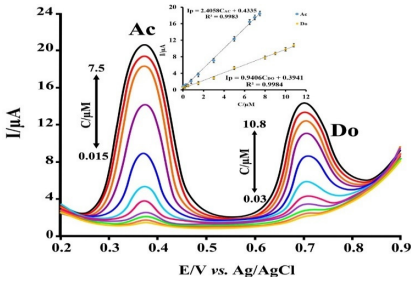

H. Khoshsafar, M. K. Rofouei, H. Bagheri, R. J. Kalbasi*